PASC23
Davos Switzerland | 26-28 June 2023

BROWN

Neural Operators for Detecting Aortic Aneurysm Contributors

Somdatta Goswami
Division of Applied Mathematics
Brown University, U.S.A.

Biophysics-Informed Machine Learning minisymposium
Platform for Advanced Scientific Computing (PASC23)

June 27, 2023

Can we predict the rupture of aneurysm?

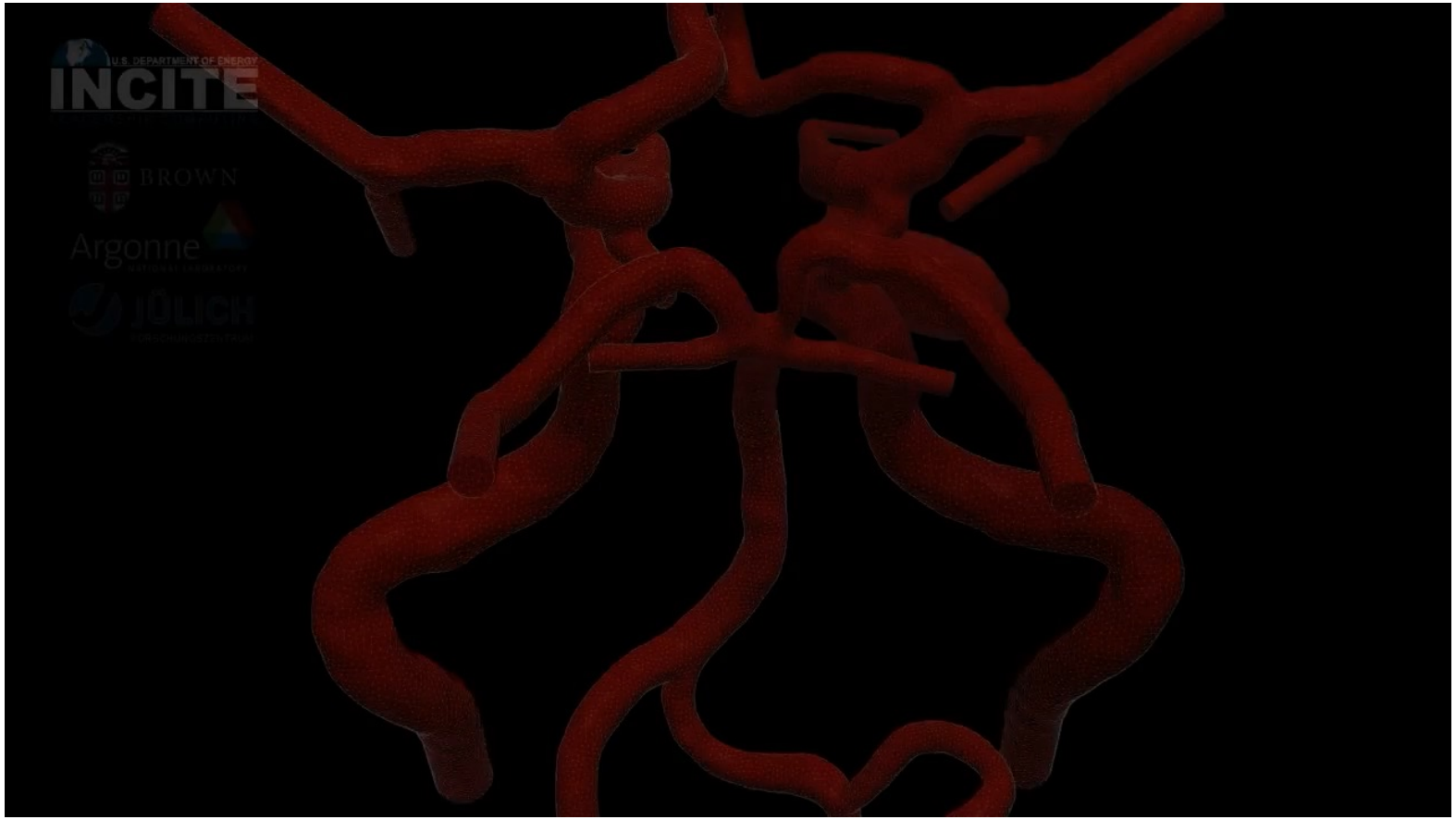

Can we predict the rupture of aneurysm?

Courtesy: Boston Children's Hospital,
J. Marsden

Data + Laws of Physics

The 5D Law: Dinky, Dirty, Dynamic, Deceptive Data

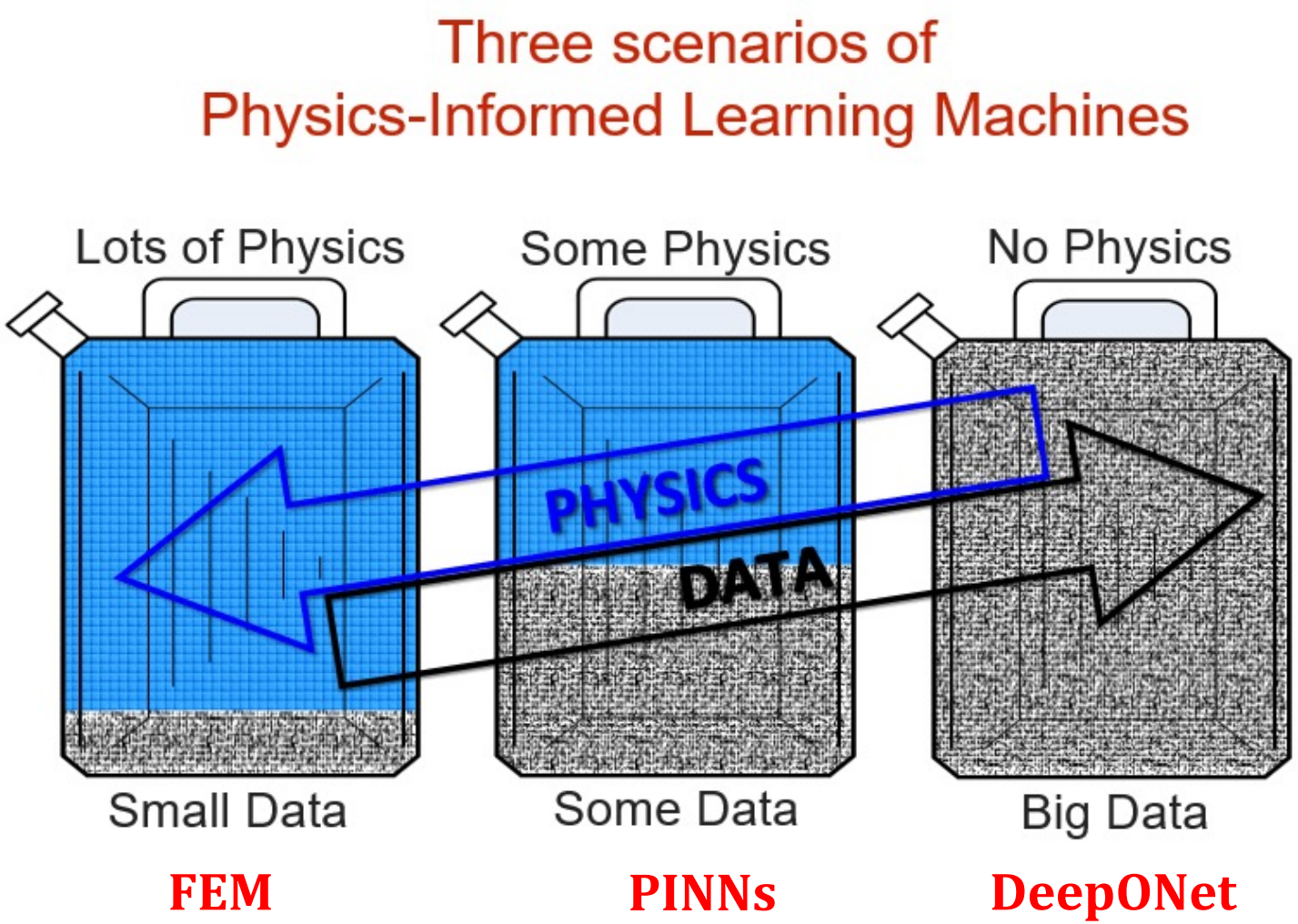

Deep Operator Networks

- Generalized Universal Approximation Theorem for Operator [Chen '95, Lu et al. '19]
- **Branch net**: Input $\{u(x_i)\}_{i=1}^m$, output: $\left[b_1, b_2, .., b_p\right]^T \in \mathbb{R}^p$
- **Trunk net**: Input y, output: $\left[t_1, t_2, .., t_p\right]^T \in \mathbb{R}^p$
- Input u is evaluated at the fixed locations $\{y_i\}_{i=1}^m$

$$G_\theta(u)(y) = \sum_{i=1}^{p} \underbrace{b_i(u(x_1), u\,(x_2), \ldots, u\,(x_m))}_{\text{branch net}} \cdot \underbrace{tr_i(y)}_{\text{trunk net}}$$

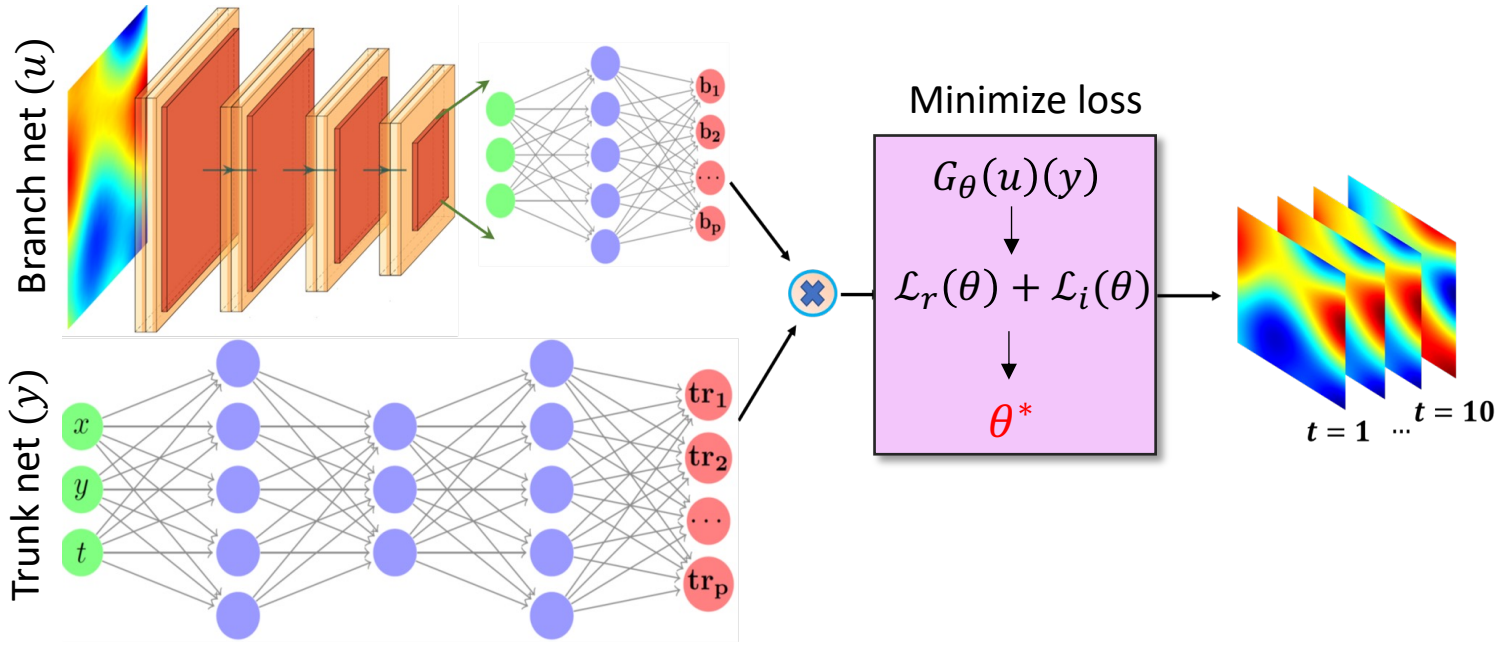

Thoracic Aortic Aneurysm

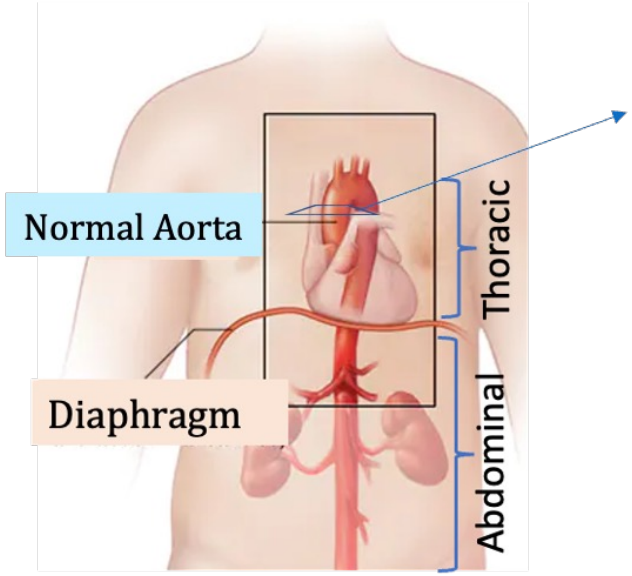

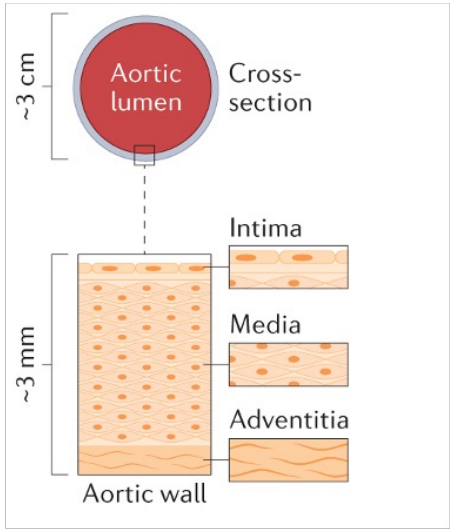

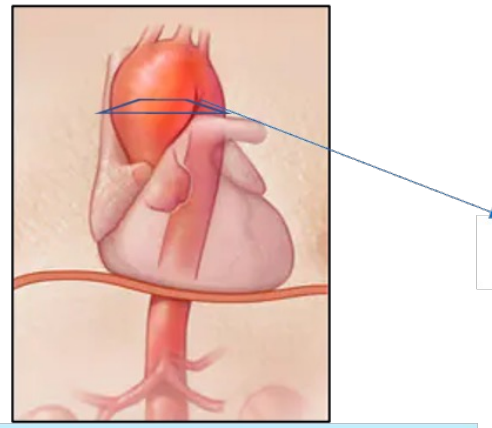

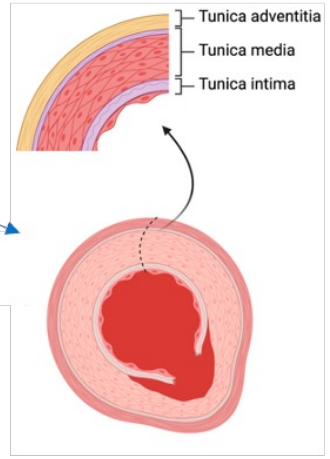

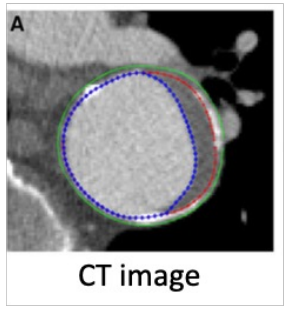

CT image

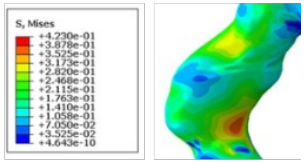

Thoracic aortic aneurysm (TAAs)

- Often grows asymptomatically and clinically silent but has 90% mortality.
- Usually, an incidental finding on imaging.
- Non-syndromic TAAs account for 95% of all TAA cases.
- Rare: with incidence of 4 – 10 per 100k people per year but yearly death rate is 6.6%.
- Rare but serious: has killed Albert Einstein, Lucille Ball, George C. Scott, and John Ritter.

TAA risk factors

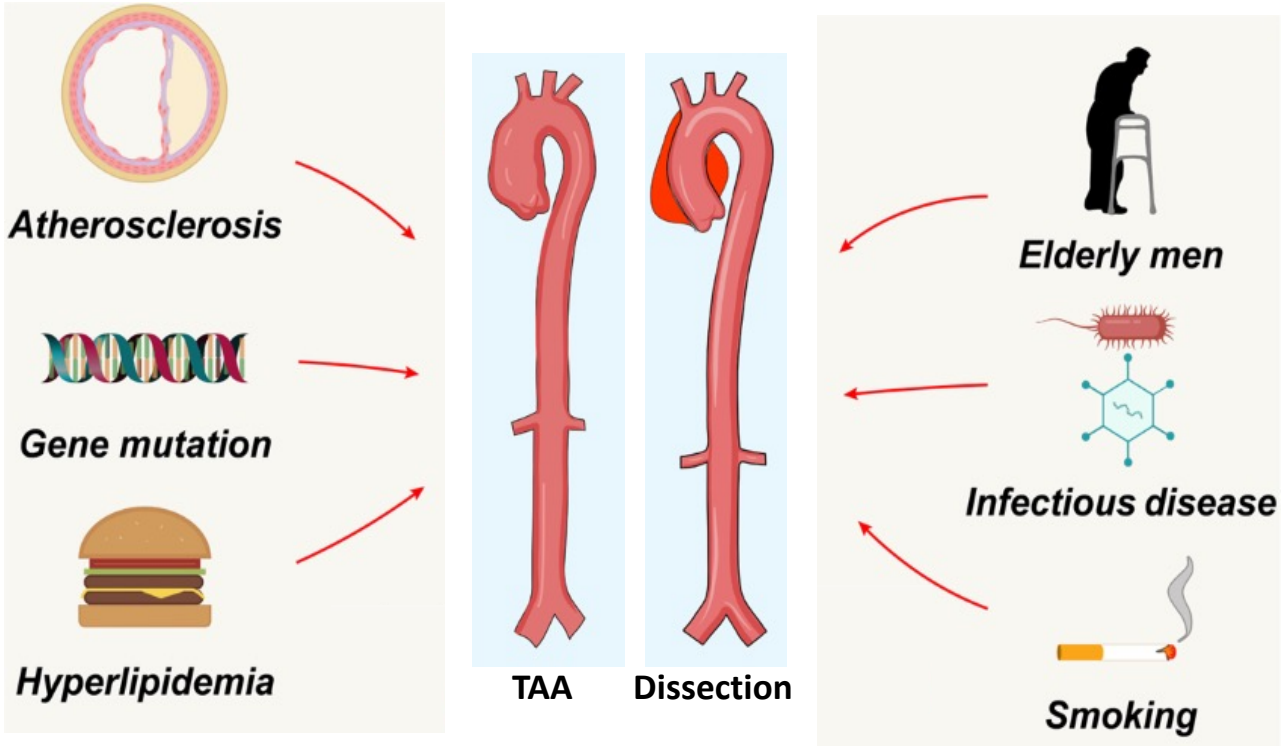

- Aortic Aneurysm is due to the inherent weakness in aortic wall layers.
- This is due to a combination of genetic factors, chronic conditions like atherosclerosis/ hyperlipidemia and other factors like smoking, infections.
- Inherent weakness + chronic stress like in hypertension → Abnormal enlargement over time.

Modeling the aneurysmal dilatation

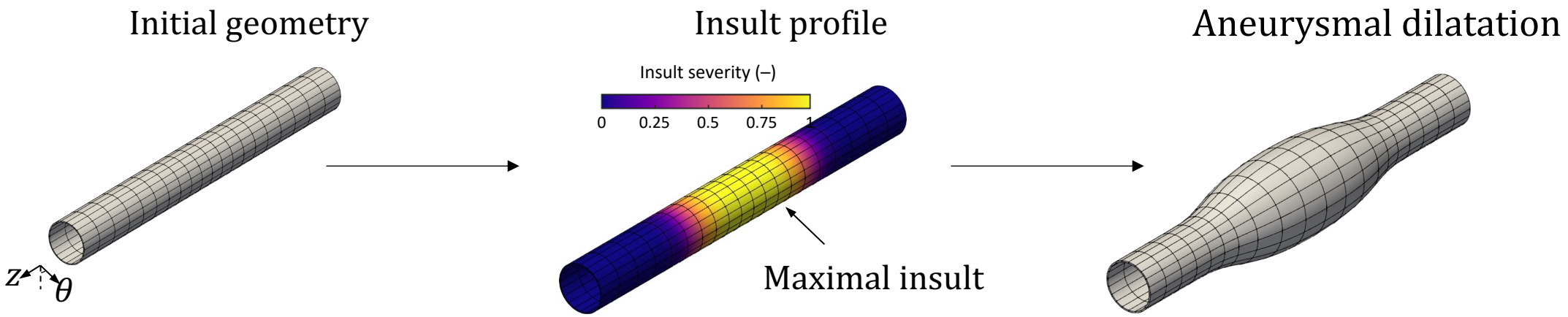

- Candidate mechanisms (insults)
  - Reduced elastic fiber integrity, C^e ⟶ Degraded elastin (fragmentation, increased voids)
  - Compromised mechanosensing, C^m ⟶ Ability of cells to sense deviations in stress from homeostatic set-point
- The insult profiles are generated considering the mechanical properties of the mouse aorta uniform wall thickness, h_o = 40 μm and luminal radius, r_o = 647 μm.

Flowchart

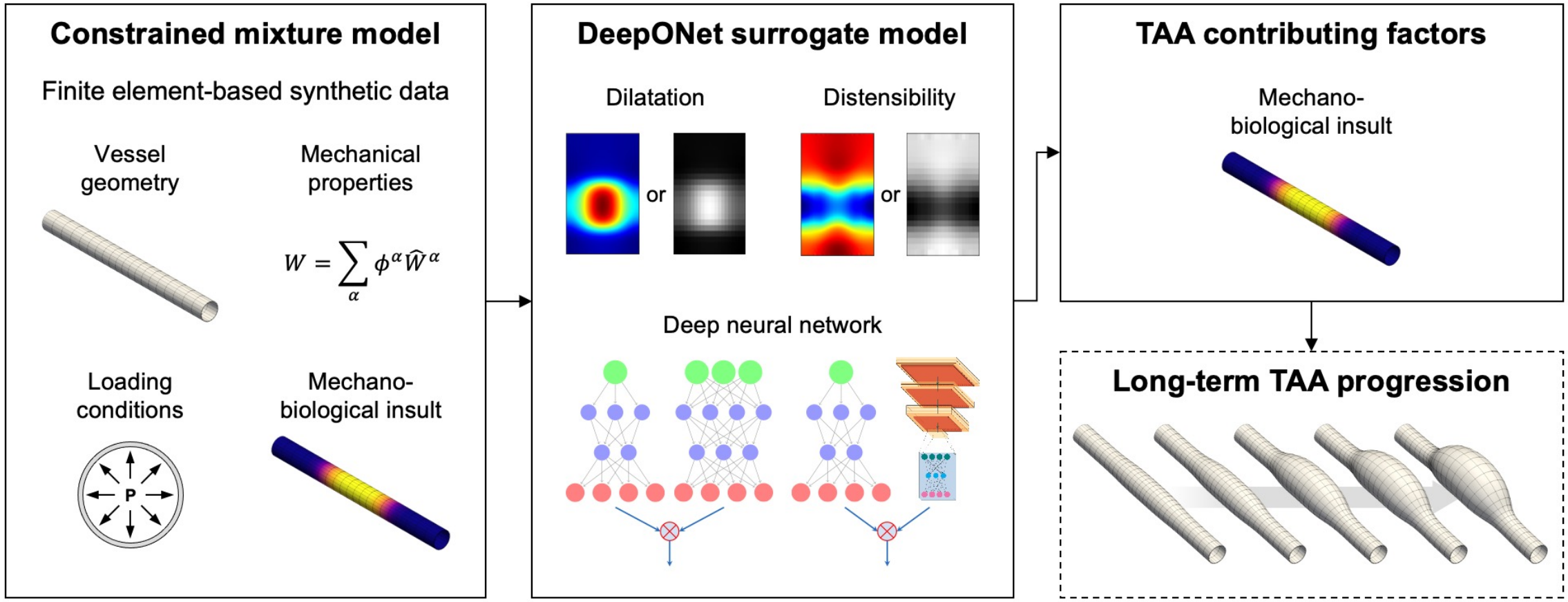
Constrained mixture model
Finite element-based synthetic data
Vessel geometry
Mechanical properties
$W = \sum_{\alpha} \phi^{\alpha} \hat{W}^{\alpha}$
Loading conditions
P
Mechano-biological insult
DeepONet surrogate model
Dilatation
Distensibility
or
or
Deep neural network
TAA contributing factors
Mechano-biological insult
Long-term TAA progression

Objective 1: Predicting the contributors

Aneurysmal dilatation

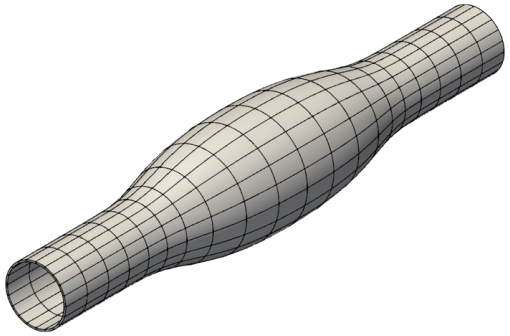

Insult profile

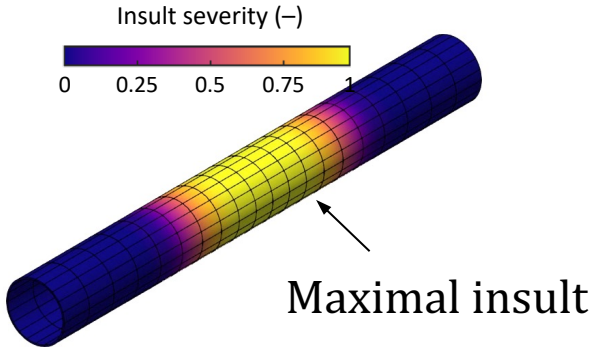

Predict the current state of patient-specific insult profile associated with any given dilatation and distensibility map

Modeling the aneurysmal dilatation

- The insult profiles are: analytically and randomly generated
- For analytically defined insult profile

$$\vartheta(z_o, \theta_o) = \vartheta_{apex} \exp\left(-\left|\frac{z_o - z_{apex}}{z_{od}}\right|^{\nu_z}\right) \exp\left(-\left|\frac{\theta_o - \theta_{apex}}{\theta_{od}}\right|^{\nu_\theta}\right)$$

Maximum insult Axial width Circumferential width

- Cases considered for normotensive and 33% hypertensive scenarios.
- The random insults are initially generated as 'latent' Gaussian random fields.

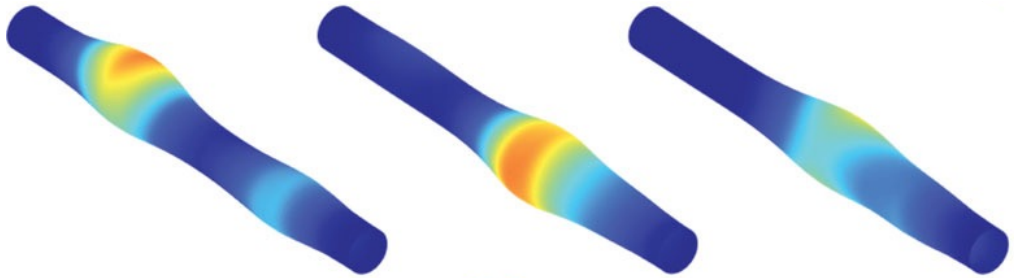

Randomly generated insults

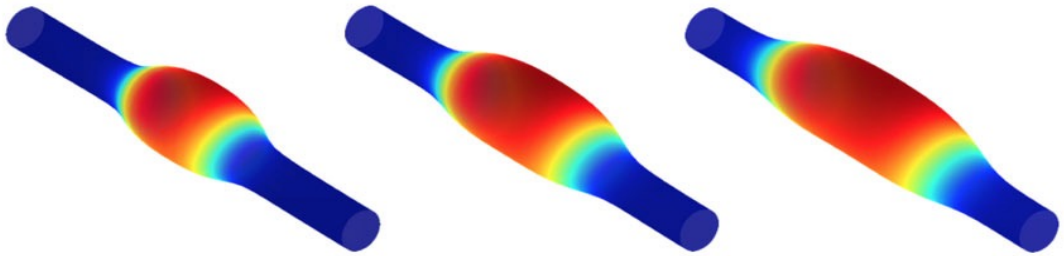

Analytically defined insults

Data Preparation

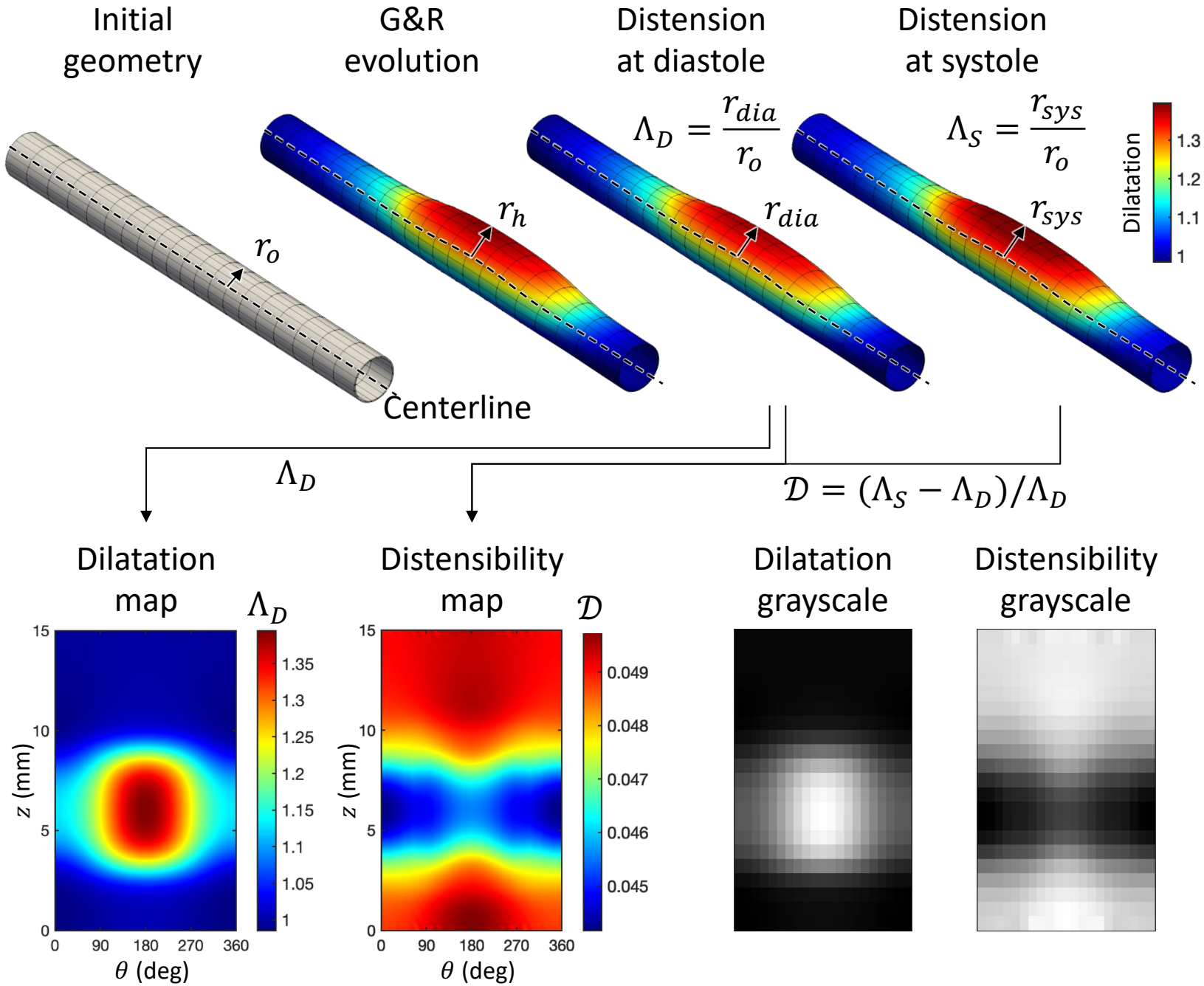

Framework 1: Using sparse measurements

- Uses sparse measurements on dilatation and distensibility maps.
- X_{Di}: co-ordinates of maximum dilation on dilation map
- X_{Ds}: co-ordinates of minimum distensibility on distensibility map
- r_1: distance(X_{Di},Q) and r_2: distance(X_{Di},Q); $Q = (0,0)$.
- Place stencils (sizes: 5×5 and 9) to obtain sensor measurements.

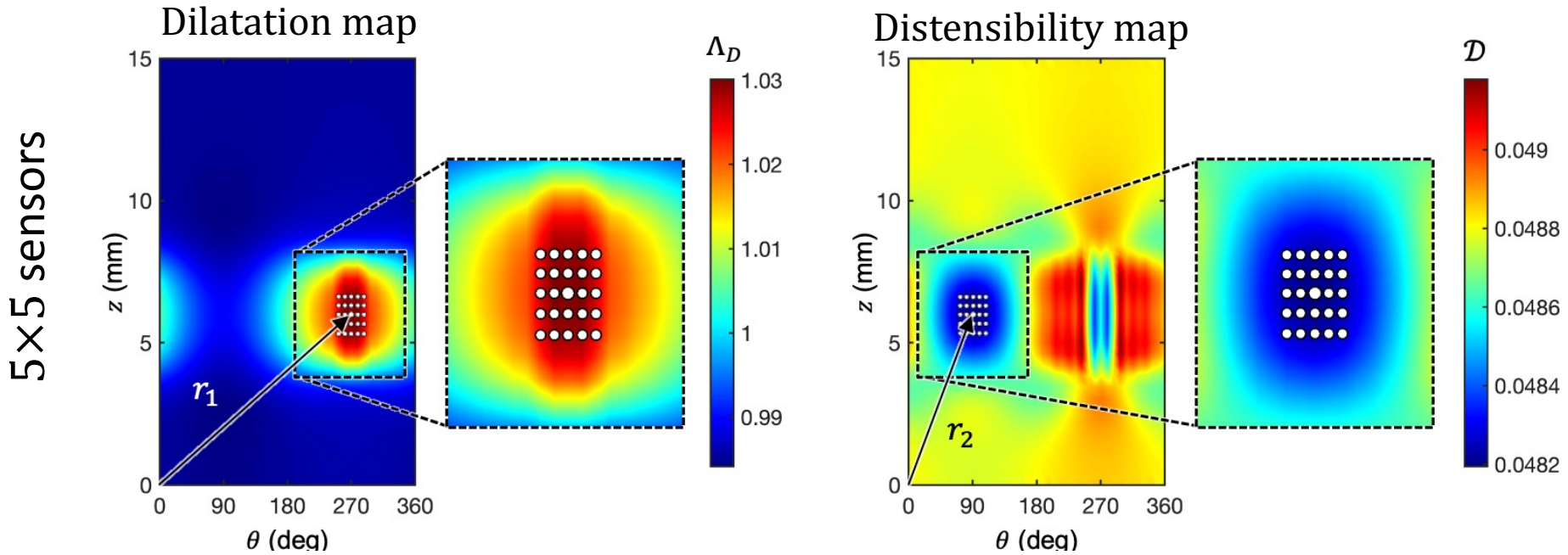

Framework 1: Using sparse measurements

- Uses sparse measurements on dilatation and distensibility maps.
- X_{Di}: co-ordinates of maximum dilation on dilation map
- X_{Ds}: co-ordinates of minimum distensibility on distensibility map
- r_1: distance(X_{Di},Q) and r_2: distance(X_{Di},Q); $Q = (0,0)$.
- Place stencils (sizes: 5×5 and 9) to obtain sensor measurements.

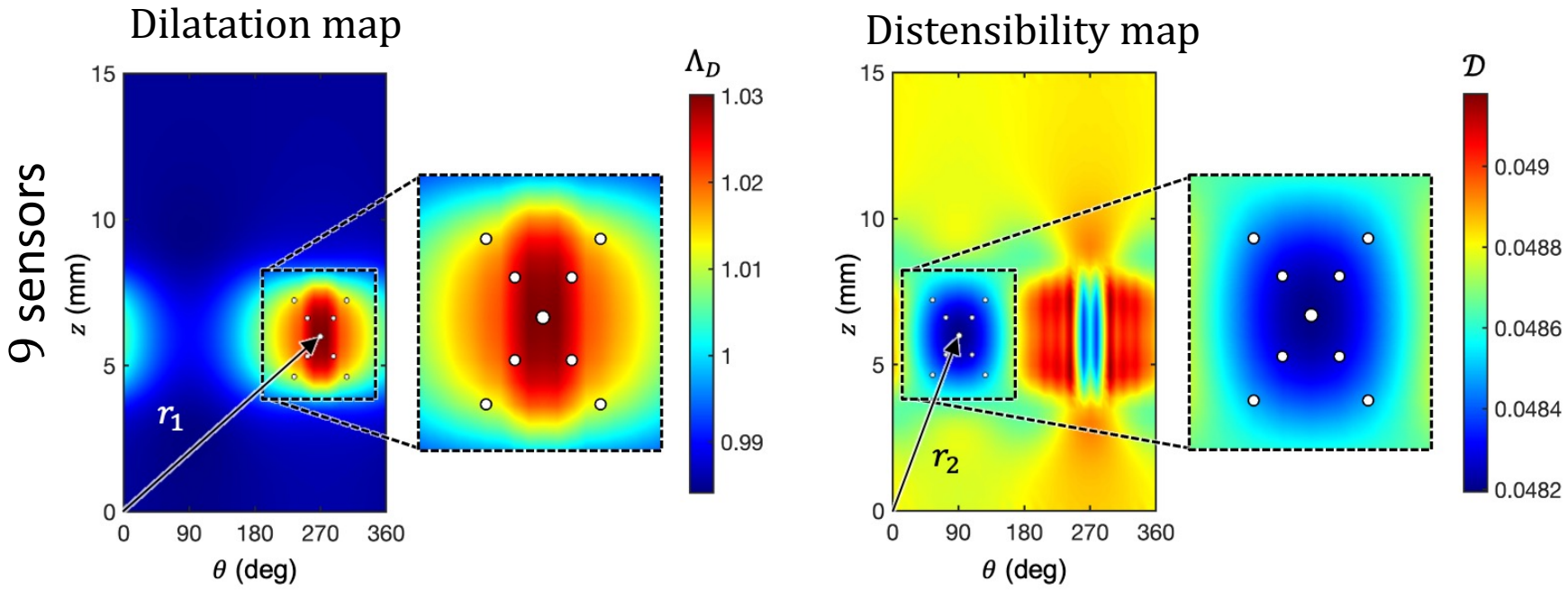

Framework 1: Using sparse measurements

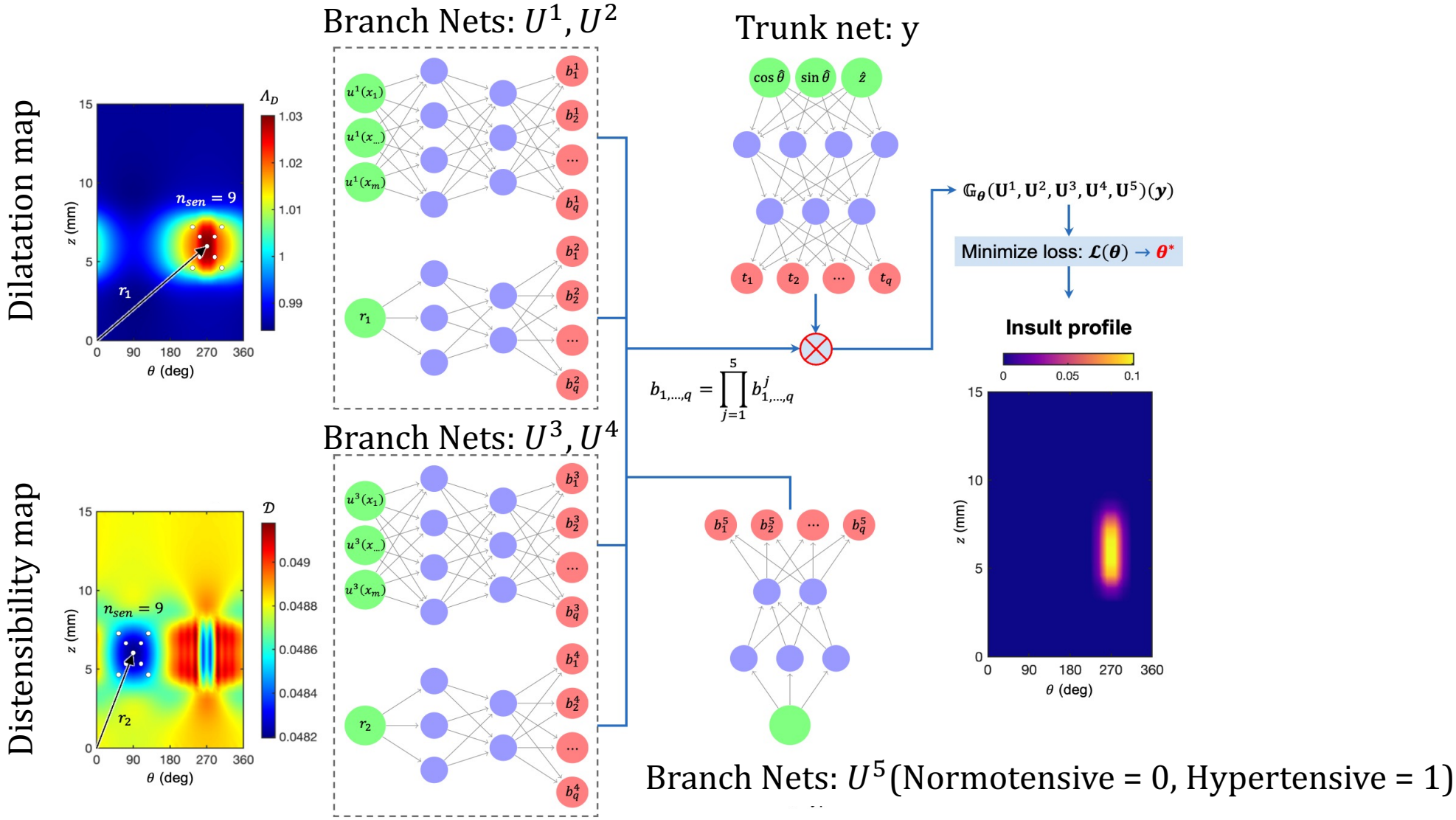

Framework 2: Using full-field images

- Original Resolution of the images: 41×40
- Input to the network: Reduced resolution 21×20
- Mimic real-world USG and MRI

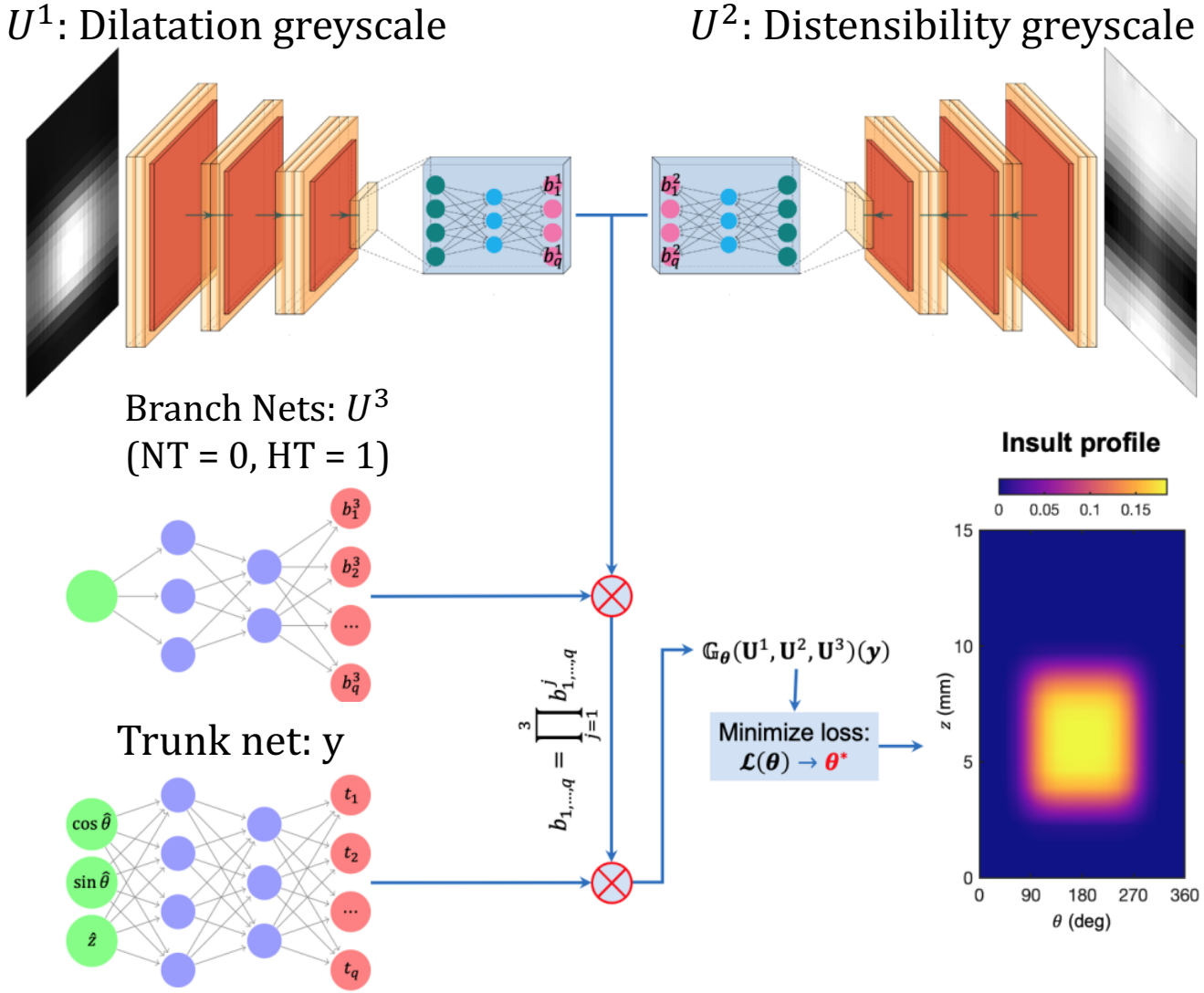

Study Cases and Results

EFI: Loss of elastic fiber integrity
MS: Loss of mechanosensing
HT: Hypertensive
NT: Normotensive

- *Case1* - EFI (NT) – 545
- *Case2* - MS (NT) – 545
- *Case3* - EFI or MS (NT) – 500
- *Case4* - MS (NT or HT) – 500
- *Case5* - EFI or MS (NT or HT) – 720

Analytically generated

- *Case6* - Randomly generated EFI or MS (NT) – 90

The numbers denote the number of training samples

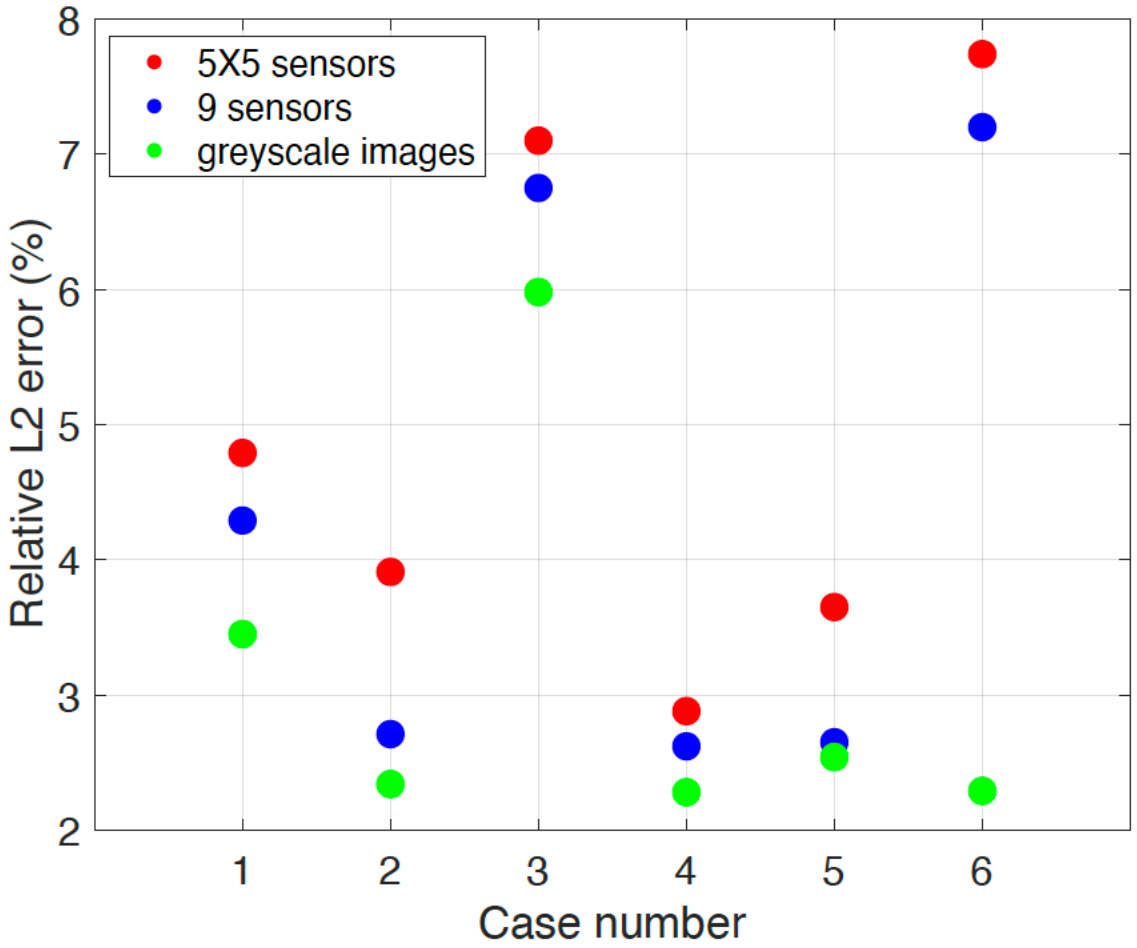

Point measurements vs noisy images

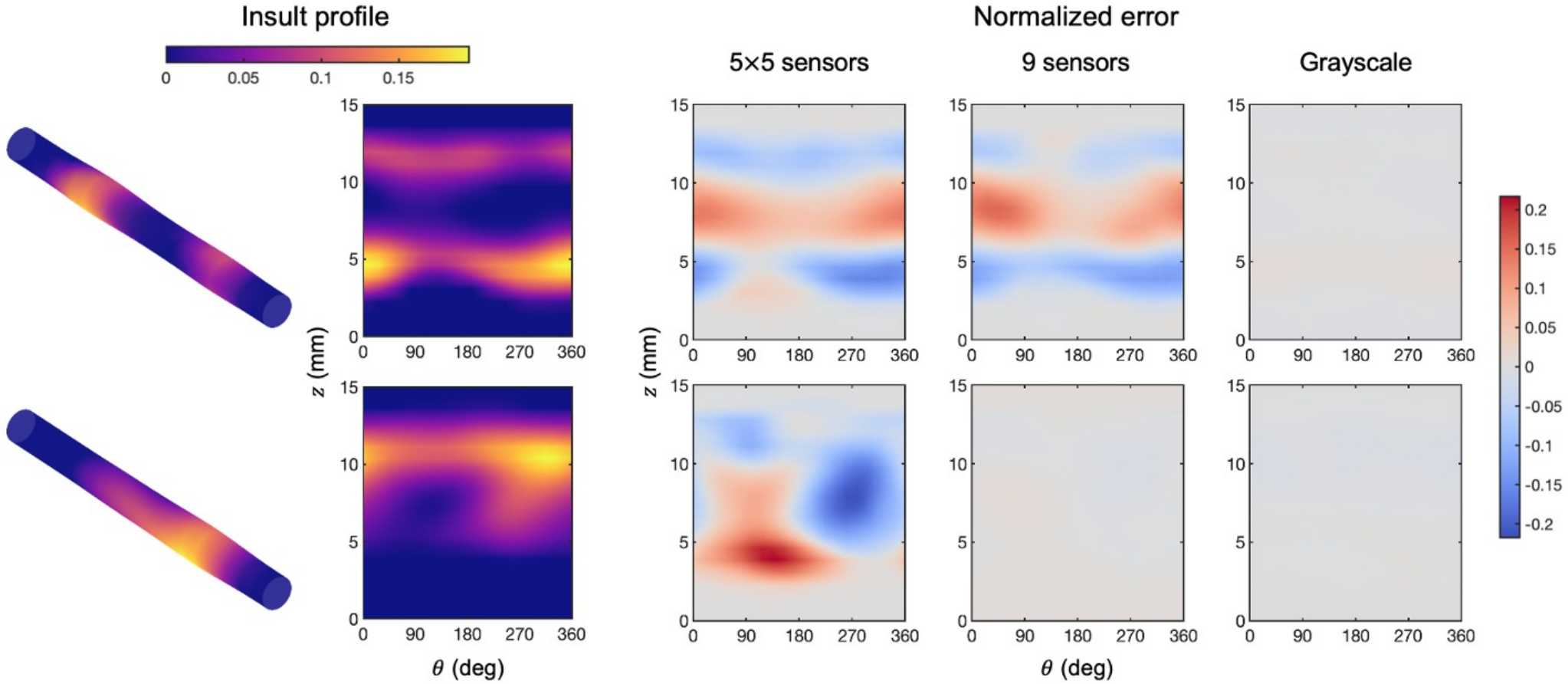

We interpret that CNNs are good de-noisers. So, even with noisy low resolution of the full field images, CNNs framework is better that accurate pointwise measurement.

Objective2: Predicting aneurysm growth and outcomes

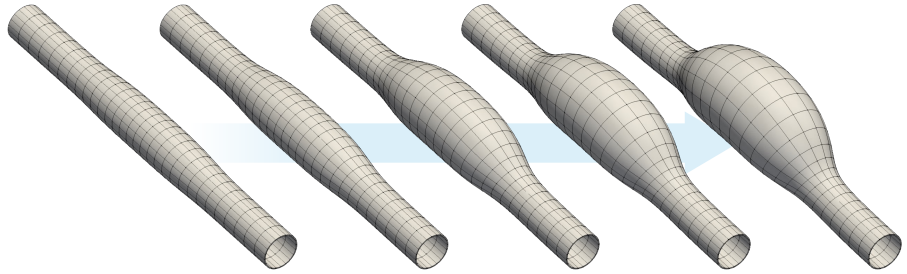

Aneurysm progression

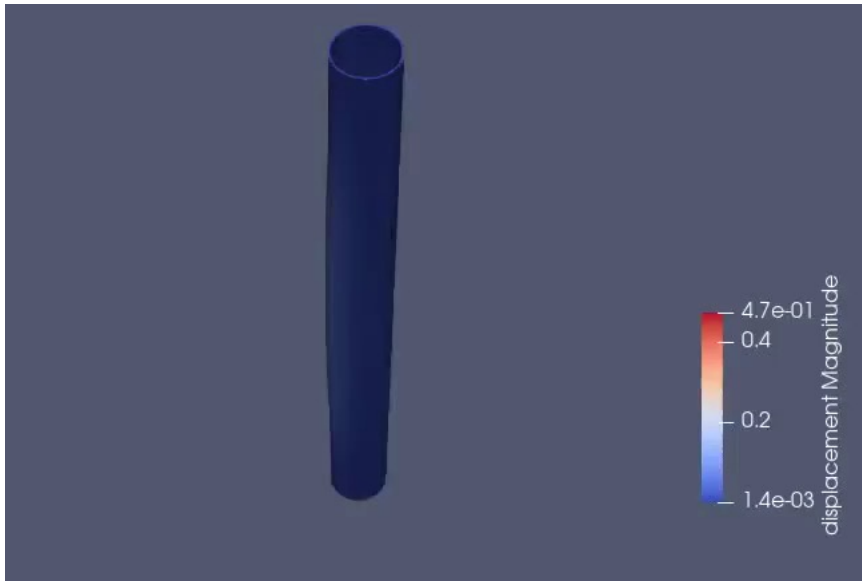

Objective 2: To predict growth of the current aneurysm over the next 6 months and 12 months , given previous & current records.

Previous records of insult profiles

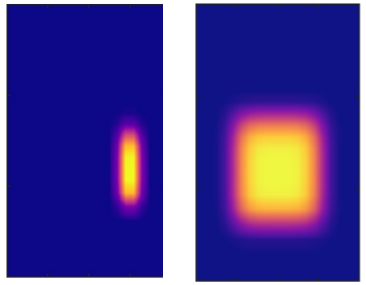

Current dilatation and distensibility map

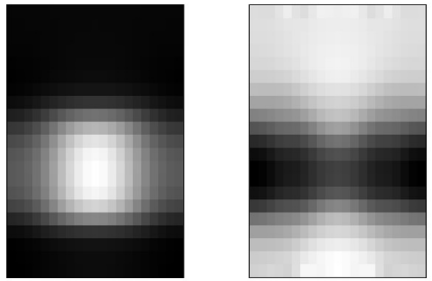

Patient specific information
(*Gender*, Marfan Syndrome, HT, etc.)

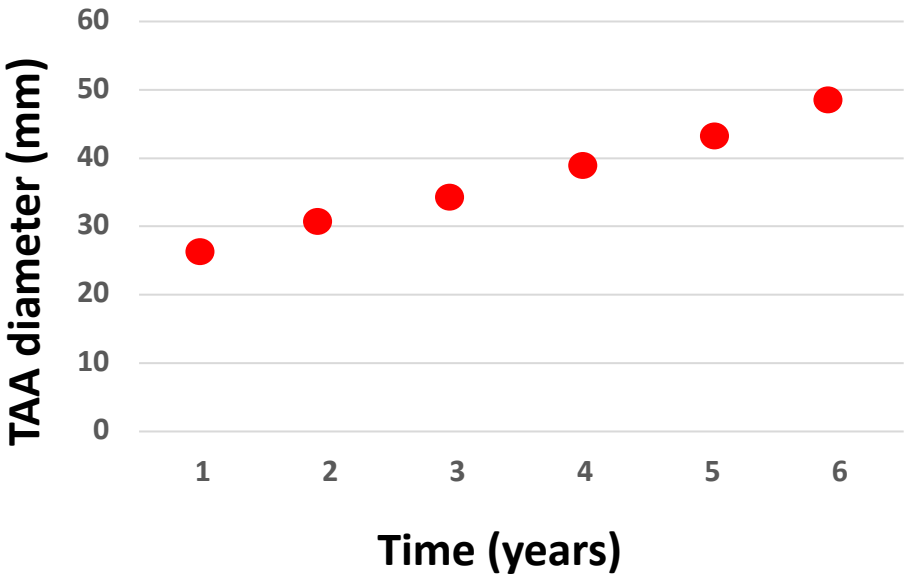

Key takeaways

- Accurate prediction of the insult profile can be achieved with the inclusion of dilatation and distensibility fields.
- Predicting insult profiles with information at 5x5 sensor locations is sufficiently accurate for cases with $\theta_{od} < 260°$ and relatively small z_{od}.
- With a wider θ_{od} and broader z_{od}, limited information within a single-spaced neighborhood near the maximum dilatation and minimum distensibility is insufficient. Hence doubly-spaced 9 sensors are beneficial in such cases.
- The choice of a CNN to train on greyscale images benefits the model in terms of not only predictive accuracy but also computational efficiency, as this framework requires fewer learnable parameters compared with the models employing FNNs.

References

1. **Goswami, S.*, Li, D. S. S.*, Rego, B. V., Latorre, M., Humphrey, J. D., & Karniadakis, G. E. (2022). Neural operator learning of heterogeneous mechanobiological insults contributing to aortic aneurysms. Journal of the Royal Society Interface, 19(193), 20220410.**
2. Lu, Lu, Pengzhan Jin, Guofei Pang, Zhongqiang Zhang, and George Em Karniadakis. (2021) Learning nonlinear operators via DeepONet based on the universal approximation theorem of operators. *Nature Machine Intelligence* 3, no. 3: 218-229.
3. Chen, T., & Chen, H. (1995). Universal approximation to nonlinear operators by neural networks with arbitrary activation functions and its application to dynamical systems. *IEEE Transactions on Neural Networks*, 6(4), 911-917.

* denotes equal contribution

The team

Dr. George Karniadakis
Professor
Brown University

Dr. Somdatta Goswami
Assistant Professor (Research)
Brown University

Dr. Jay Humphrey
Professor
Yale University

Dr. David Li
Postdoctoral Researcher
Yale University

Funding:

NATIONAL INSTITUTES OF HEALTH
NIH
UNITED STATES OF AMERICA

Computing support:

CCV
@Brown

Thank you!

Contact: somdatta_goswami@brown.edu